Simple microwave field imaging technique using hot atomic vapor cells

Pascal Böhi, and Philipp Treutlein

Citation: Appl. Phys. Lett. **101**, 181107 (2012); doi: 10.1063/1.4760267

View online: https://doi.org/10.1063/1.4760267

View Table of Contents: http://aip.scitation.org/toc/apl/101/18

Published by the American Institute of Physics

Simple microwave field imaging technique using hot atomic vapor cells

Pascal Böhi and Philipp Treutlein[a)]
Departement Physik, Universität Basel, Klingelbergstrasse 82, 4056 Basel, Switzerland

(Received 20 July 2012; accepted 3 October 2012; published online 29 October 2012)

We demonstrate a simple technique for microwave field imaging using alkali atoms in a vapor cell. The microwave field to be measured drives Rabi oscillations on atomic hyperfine transitions, which are detected in a spatially resolved way using a laser beam and a camera. Our vapor cell geometry enables single-shot recording of two-dimensional microwave field images with 350 μm spatial resolution. Using microfabricated vapor cell arrays, a resolution of a few micrometers seems feasible. All vector components of the microwave magnetic field can be imaged. Our apparatus is simple and compact and does not require cryogenics or ultra-high vacuum. © *2012 American Institute of Physics*. [http://dx.doi.org/10.1063/1.4760267]

Integrated microwave circuits are an essential part of modern communication technology and scientific instrumentation. For development and testing of such circuits, a technique for high-resolution imaging of microwave field distributions is needed. Different methods have been investigated for this purpose,[1] but a truly satisfactory standard technique does not exist. We recently demonstrated a technique that uses laser-cooled ultracold atoms for microwave field imaging.[2,3] This technique is non-invasive, parallel and therefore fast, offers high spatial and microwave field resolution, and allows the reconstruction of field amplitudes and phases.

Although significant progress has been made in simplifying ultracold atom experiments,[4] the requirements for ultra-high vacuum and laser cooling still represent a challenge for microwave field imaging applications in industry. From a practical point of view, it would be very attractive to use thermal atoms in a vapor cell instead, at room temperature or moderately heated. Atomic vapor cells already find widespread use in commercial atomic clocks,[5] magnetometers for static and radio-frequency fields,[6–10] and are investigated as a potential microwave power standard.[11,12] In microwave field imaging, however, high spatial resolution is required, and the fast thermal motion of the atoms presents a serious challenge.

Here, we demonstrate a technique for microwave field imaging that uses an ensemble of near room-temperature atoms in a vapor cell.[13] Similar to the technique using ultracold atoms,[2] it relies on position-resolved detection of microwave-driven Rabi oscillations between atomic hyperfine states. It provides single-shot 2D imaging, reconstruction of amplitudes and phases, and can be made frequency-tunable. Since the measured Rabi frequencies only depend on the local microwave field strength and well-known atomic constants, the method is intrinsically calibrated. While the proof-of-principle experiment reported here does not yet reach the same spatial resolution as the previous technique using ultracold atoms,[2] we point out how micrometer-scale spatial resolution can be reached using an array of microfabricated vapor cells.[14–17] The experimental setup for our method is simple, requiring neither cryogenics nor ultra-high vacuum, which makes it promising for the characterization of microwave circuits in real-life applications.

The experimental setup is shown in Fig. 1(a): A vapor cell is connected to an atomic reservoir, a vacuum pump, and a buffer gas reservoir. In general, any atomic species with microwave transitions that can be read out optically can

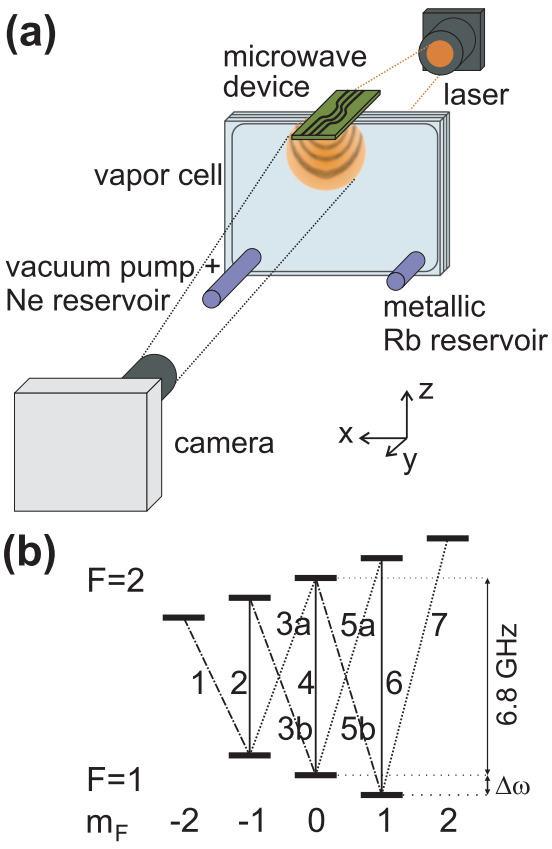

FIG. 1. (a) Experimental setup. The microwave device under test is mounted next to an atomic vapor cell, which is connected to a Rb reservoir, a vacuum pump, and a Ne buffer gas reservoir. A laser images the hyperfine state distribution of the ^{87}Rb atoms in the cell onto a CCD camera. The cell is surrounded by magnetic field coils and sits inside an oven (not shown). (b) Ground-state hyperfine levels $|F, m_F\rangle$ of ^{87}Rb in a weak static magnetic field. The microwave transitions $i = 1 \ldots 7$ are indicated; transitions 3a + b and 5a + b are degenerate. The laser light selectively images the $F = 2$ state.

a)E-mail: philipp.treutlein@unibas.ch.

be used. In our specific example, we use ^{87}Rb atoms in a natural-abundance Rb vapor. Neon buffer gas is added to slow down the diffusion of Rb atoms through the cell.[18] This enhances the spatial resolution of our field imaging method. The cell has a 2D geometry (much thinner than wide) to allow recording of a 2D image of the microwave field. It consists of two quartz glass plates that are epoxy-glued to a 3 mm thick glass frame. The microwave device to be characterized is mounted at the outside of the cell. It can be moved along the y-direction so that 2D images of the microwave field can be taken in any desired cross-section of the device. A diode laser provides 780 nm light for optical pumping and for absorption imaging of the atomic hyperfine state distribution onto a charge-coupled device (CCD) camera. The vapor cell and microwave device are placed inside an oven with two windows for optical access. Heating the cell increases the Rb vapor density and thereby enhances laser absorption. We point out that our system can also be operated at ambient temperature, albeit at a lower signal-to-noise level. A set of Helmholtz coils is used to apply a homogeneous static magnetic field $\mathbf{B}_0$. Figure 1(b) shows the ground-state hyperfine structure of ^{87}Rb in this field. The Zeeman effect results in a splitting of the microwave transition frequencies ω_i $(i=1\ldots7)$ connecting the m_F sublevels of the $F=1$ state to that of the $F=2$ state. For $B_0 \ll 0.1\,\mathrm{T}$, we have $\omega_i = 2\pi \times 6.835\,\mathrm{GHz} + (i-4)\Delta\omega$, where $\Delta\omega = \mu_B B_0/2\hbar$ is the Larmor frequency.

The experimental sequence starts by applying a 100 ms pulse of laser light to the atoms, which resonantly couples the $F=2$ ground state to the Doppler-broadened excited-state manifold of the ^{87}Rb D_2 transition. This pulse optically pumps atoms from $F=2$ to $F=1$, creating a population imbalance between the ground states.[18,19] Next, we turn on the microwave field to be imaged for a duration dt_{mw}, with frequency $\omega_{\mathrm{mw}} = \omega_i$ tuned to resonance with one of the transitions $i=1$, 4, 7. The microwave field drives Rabi oscillations[19] of frequency $\Omega_i(\mathbf{r})$ on the resonant transition, resulting in a modulation of the atomic population in $F=2$ and a corresponding modulation of the optical density OD of the vapor of

$$\Delta\mathrm{OD}(x,z) \propto \sin^2\left[\frac{1}{2}|\Omega_i(x,y_0,z)|dt_{\mathrm{mw}}\right],$$

where y_0 is the y-position of the cell. After the microwave pulse, we apply another laser pulse and image the light transmitted through the cell onto the camera. The duration $dt_{\mathrm{im}} = 10\,\mu\mathrm{s}$ of this imaging pulse is short enough so that optical pumping can be neglected. We determine $\Delta\mathrm{OD}(x,z) = -\ln[I_{\mathrm{mw}}(x,z)/I_{\mathrm{ref}}(x,z)]$, where I_{mw} (I_{ref}) is the transmitted intensity with (without) the microwave pulse applied, see Fig. 2(a). We record Rabi oscillations by varying dt_{mw} and/or the power P_{mw} on the microwave device ($\Omega_i \propto \sqrt{P_{\mathrm{mw}}}$) and extract $\Omega_i(x,y_0,z)$ for each pixel of the CCD image by a sinusoidal fit.[2]

The Rabi frequencies $\Omega_i(\mathbf{r})$ are proportional to specific components of the microwave magnetic field $\mathcal{B}(\mathbf{r},t) = \frac{1}{2}[\mathbf{B}(\mathbf{r})e^{-i\omega_{\mathrm{mw}}t} + \mathbf{B}^*(\mathbf{r})e^{i\omega_{\mathrm{mw}}t}]$. For ^{87}Rb, we have, e.g.,

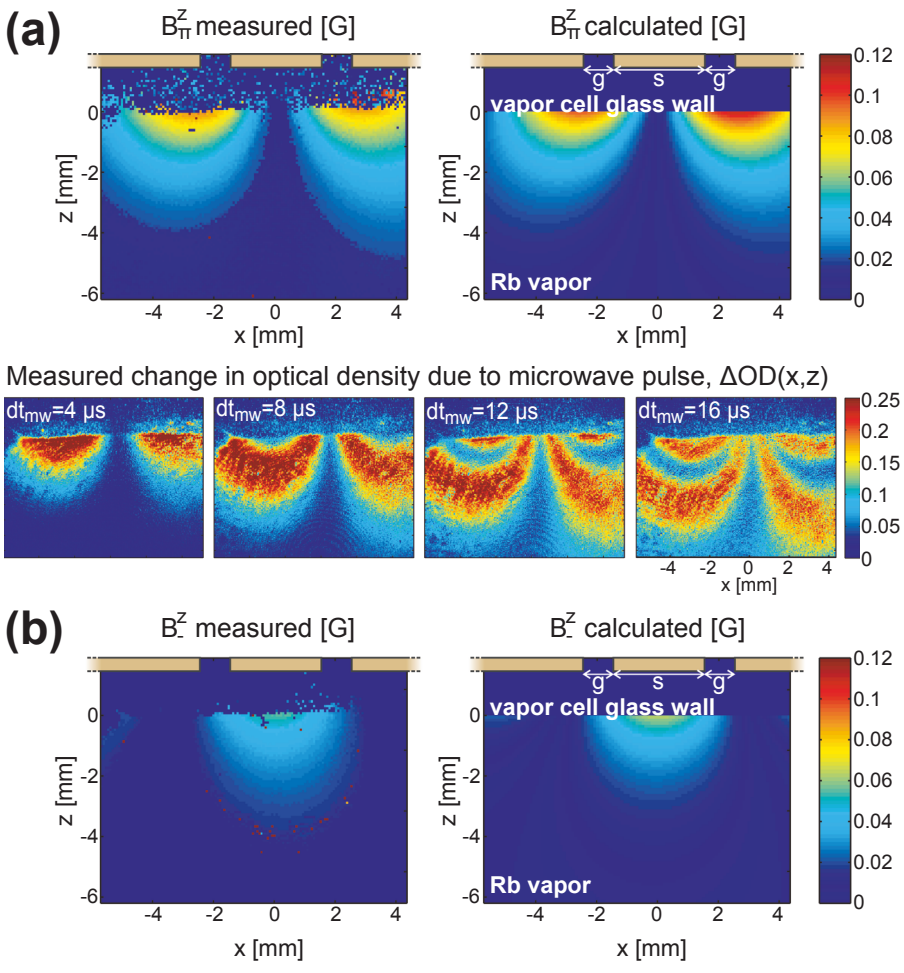

FIG. 2. Images of two exemplary microwave magnetic field components near a CPW and comparison to a simulation. (a) Top: Spatial distribution of B^z_π, i.e., the B_π polarization component for $\mathbf{B}_0$ pointing along z. For this measurement, we probed the transition $|1,0\rangle \rightarrow |2,0\rangle$ $(i=4)$ at $B_0 = 0.15\,\mathrm{mT}$. On top of the vapor cell, the CPW is indicated ($s=3\,\mathrm{mm}$, $g=1\,\mathrm{mm}$, wire thickness not to scale). The vapor cell glass wall prevents imaging at distances $<1.5\,\mathrm{mm}$ from the CPW. Bottom: Corresponding raw data of the change in optical density $\Delta\mathrm{OD}(x,z)$ for different values of dt_{mw}. This data were used to extract B^z_π. (b) Distribution of B^z_- measured on the transition $|1,-1\rangle \rightarrow |2,-2\rangle$ $(i=1)$.

$$\hbar\Omega_1(\mathbf{r}) = -\sqrt{3}\,\mu_B B_-(\mathbf{r}) e^{-i\phi_-(\mathbf{r})},$$

$$\hbar\Omega_4(\mathbf{r}) = -\mu_B B_\pi(\mathbf{r}) e^{-i\phi_\pi(\mathbf{r})},$$

$$\hbar\Omega_7(\mathbf{r}) = \sqrt{3}\,\mu_B B_+(\mathbf{r}) e^{-i\phi_+(\mathbf{r})}.$$

Here, B_π and ϕ_π are the real-valued amplitude and phase of the component of $\mathbf{B}$ parallel to $\mathbf{B}_0$, and $\mathbf{B}_+, \phi_+$ ($\mathbf{B}_-, \phi_-$) are the corresponding quantities for the right-handed (left-handed) circular polarization component in the plane perpendicular to $\mathbf{B}_0$.

The components of the complex microwave magnetic field vector $\mathbf{B}(\mathbf{r})$ can be determined by measuring Rabi frequencies on different transitions. A single measurement yields the amplitude of one component, but not the phase. To determine amplitudes as well as relative phases of all components, sequential measurements of $B_\pi(\mathbf{r})$, $B_+(\mathbf{r})$, and $B_-(\mathbf{r})$ with the static field $\mathbf{B}_0$ pointing along x, y, and z are sufficient. From these nine measurements, $\mathbf{B}(\mathbf{r})$ can be reconstructed up to a global phase, as explained in Ref. 2. It is also possible to determine the spatial dependence of the global phase using an interferometric method.[2]

To demonstrate our method, we have imaged the microwave field of a simple coplanar waveguide (CPW) with finite ground wires, see Fig. 2. The CPW is made of 35 μm thick copper wires ($s = 3$ mm, $g = 1$ mm, ground wires 8 mm wide) on a 1.5 mm thick FR-4 substrate and has a characteristic impedance of 70 Ω. We operate the vapor cell with $p = 10$ mbar of Ne buffer gas at a temperature of $T \approx 115$°C. After optical pumping with a laser intensity of $I_0 = 0.2\,\mathrm{mW/cm^2}$, we measure an optical density OD ≈ 0.5. The microwave pulse is applied with $P_{\mathrm{mw}} \approx 5$ W and dt_{mw} is varied between 1 and 30 μs. Figure 2(a) (bottom) shows the observed change in optical density $\Delta\mathrm{OD}(x,z)$ for a specific component of the MW field and different values of dt_{mw}. The smallest spatial features on the image with $dt_{\mathrm{mw}} = 16\,\mu$s have a size of 350 μm (peak-to-valley). This is comparable to the calculated r.m.s. distance $\Delta x = \sqrt{2Ddt_{\mathrm{mw}}} = 320\,\mu$m that a Rb atom diffuses during the microwave pulse. Here, $D = D_0 p_0/p$ is the diffusion coefficient for Rb in Ne at pressure p, and $D_0 = 0.31\,\mathrm{cm^2/s}$ is the same quantity at atmospheric pressure p_0.[18] For larger values of dt_{mw}, the images start to blur as Δx grows and the spatial modulations in $\Delta\mathrm{OD}(x,z)$ get narrower. The vapor cell glass wall prevents imaging at distances <1.5 mm from the CPW. In an optimized design, the wall thickness would be reduced to allow for imaging at tens of micrometers from the chip. Two microwave field components reconstructed from such images are shown in Figs. 2(a) and 2(b) in comparison with a simulation.[20] The simulation agrees well with the measurement if we allow for an 8% asymmetry between the two ground wire currents. While these experiments are a proof-of-principle demonstration using a simple and macroscopic prototype device, much smaller microwave circuits could be characterized with our method as discussed below.

After a few months, the Rb in our cell oxidized. We speculate that this is due to the epoxy used to glue our cell (EPO-TEK 353ND). Recent experiments indicate that only certain epoxy glues are compatible with Rb vapor.[21] Another possible explanation is contamination of the buffer gas. The optical density of our cell at $T \approx 115$ °C drops from OD ≈ 5 without buffer gas to OD ≈ 0.5 at $p = 10$ mbar. Pressure broadening due to buffer gas is known to decrease optical density,[22] but the decrease we observe is much higher than expected for pure Ne. We are confident that these issues can be resolved using a different vapor cell fabrication technique. As reported in Ref. 15, microfabricated alkali vapor cells with Ne buffer gas pressures up to 200 mbar show very good long-term stability even at elevated temperatures.

One way to increase the spatial resolution of our field imaging method is to use a cell with higher buffer gas pressure to more effectively slow down the Rb motion. Neon is particularly well suited as buffer gas because of its small pressure broadening coefficient[22] and small cross section for hyperfine relaxation.[18] Microfabricated alkali vapor cells with Ne at $p = 100$ mbar have been developed for miniaturized atomic clocks.[15] In such a cell, the atoms diffuse only $\Delta x = 25\,\mu$m during $dt_{\mathrm{mw}} = 1\,\mu$s. This suggests that a transverse spatial resolution of several tens of micrometers can be achieved using buffer gas. In a cell of 200 μm thickness at $T = 100$°C, the Rb vapor has OD = 0.3, including pressure broadening.[22,23] Hyperfine relaxation is estimated to occur on a timescale of several μs, dominated by wall collisions.[18]

Even higher spatial resolution can be obtained by confining the atoms in an array of micromachined cells fabricated into a substrate.[14–17] Each microcell acts as a pixel of the microwave field image. Using recently developed high-temperature antirelaxation coatings,[24] the hyperfine state of the atoms can survive $\approx$850 atom-wall collisions at cell temperatures up to 170 °C. This allows for interaction times up to $dt_{\mathrm{mw}} \simeq 850\,d/\bar{v} = 13\,\mu$s in a cubic cell of side length $d = 5\,\mu$m without buffer gas, where the atoms move ballistically with average thermal velocity $\bar{v} = 320\,\mathrm{m/s}$ at $T = 145$ °C. Micrometer-scale spatial resolution is thus within reach. The optical density is OD = 0.2 and Rb spin exchange relaxation is expected to occur on a time scale of 15 μs.[18] A small amount of Rb could be deposited in each microcell during fabrication. Alternatively, the cells could be connected by thin trenches in the substrate to a single Rb reservoir.

We now estimate the microwave field sensitivity that can be obtained with such microcells. Assuming a photon-shot-noise-limited imaging system and $dt_{\mathrm{im}} = 10\,\mu$s, the smallest optical density change that can be resolved on a pixel of area $A = d^2$ is $\Delta\mathrm{OD}_{\mathrm{min}} = \sqrt{\hbar\omega_L/I_0 A\,dt_{\mathrm{im}}} = 0.02$, where ω_L is the laser frequency. This implies that a Rabi frequency as small as $\Omega_{\mathrm{min}} \simeq (2/dt_{\mathrm{mw}})\sqrt{\Delta\mathrm{OD}_{\mathrm{min}}/\mathrm{OD}} = 2\pi \times 9\,\mathrm{kHz}$ could be detected in a single shot. This corresponds to a microwave magnetic field amplitude of a few hundred nT, which arises, e.g., at a distance of 5 μm from a microwave guide carrying a signal of $P_{\mathrm{mw}} \simeq 7$ nW. In general, a higher spatial resolution implies a lower microwave field resolution, because both the maximal dt_{mw} is shorter and the area A over which the image is integrated is smaller.

Microwave field imaging at 6.8 GHz is useful, e.g., for the characterization of C-band GaN power amplifiers or scientific applications such as atom chip design.[20] However, our method is not restricted to fixed frequency, since the transition frequencies ω_i can be tuned by means of the static magnetic field B_0. Frequencies up to 50 GHz are accessible with standard laboratory fields up to $B_0 = 1.6$ T. For $B_0 > 0.1$ T,

the atoms enter the Paschen-Back regime, where the hyperfine transition matrix elements change. Nevertheless, a full reconstruction of the microwave field is still possible. At the low-frequency end, the zero-field hyperfine splitting sets a limit. Atoms with smaller hyperfine splitting such as ^{85}Rb (3.0 GHz) or ^{39}K (0.5 GHz) give access to low frequencies.

The simplicity of our method should allow the construction of integrated microwave field imaging devices. We envision future devices consisting of micromachined vapor cell arrays with integrated electromagnets to tune the transition frequencies to the desired values and optical waveguides delivering the light for optical pumping and imaging.

We thank T. W. Hänsch for inspiring discussions, M. F. Riedel for help with the experimental setup, A. Horsley for discussions on vapor cells, and G.-X. Du for careful reading of the manuscript. This work is supported by the EU project AQUTE and the Swiss National Science Foundation.

[1]S. Sayil, D. V. Kerns, and S. E. Kerns, IEEE Trans. Instrum. Meas. **54**, 2082 (2005).
[2]P. Böhi, M. F. Riedel, T. W. Hänsch, and P. Treutlein, Appl. Phys. Lett. **97**, 051101 (2010), see also supplementary material at http://dx.doi.org/10.1063/1.3470591 for details on reconstruction of the microwave field vector.
[3]P. Böhi, M. F. Riedel, T. W. Hänsch, and P. Treutlein, "Method and device for sensing microwave magnetic field polarization components," U.S. patent application 12/729,812 (2010).
[4]D. M. Farkas, K. M. Hudek, E. A. Salim, S. R. Segal, M. B. Squires, and D. Z. Anderson, Appl. Phys. Lett. **96**, 093102 (2010).
[5]F. G. Major, *The Quantum Beat*, 2nd ed. (Springer, New York, 2010).
[6]D. Budker and M. Romalis, Nat. Phys. **3**, 227 (2007).
[7]E. E. Mikhailov, I. Novikova, M. D. Havey, and F. A. Narducci, Opt. Lett. **34**, 3529 (2009).
[8]I. M. Savukov, S. J. Seltzer, M. V. Romalis, and K. L. Sauer, Phys. Rev. Lett. **95**, 063004 (2005).
[9]A. Ben-Amar Baranga, S. Appelt, C. J. Erickson, A. R. Young, and W. Happer, Phys. Rev. A **58**, 2282 (1998).
[10]A. R. Young, S. Appelt, A. Ben-Amar Baranga, C. Erickson, and W. Happer, Appl. Phys. Lett. **70**, 3081 (1997).
[11]J. C. Camparo, Phys. Rev. Lett. **80**, 222 (1998).
[12]J. Sedlacek, A. Schwettmann, H. Kübler, R. Löw, T. Pfau, and J. P. Shaffer, Nature Phys. advance online publication (2012), http://dx.doi.org/10.1038/nphys2423.
[13]P. Böhi, P. Treutlein, M. F. Riedel, and T. W. Hänsch, "Simple microwave field imaging device," European patent application EP12161027 (2012).
[14]T. Baluktsian, C. Urban, T. Bublat, H. Giessen, R. Löw, and T. Pfau, Opt. Lett. **35**, 1950 (2010).
[15]M. Hasegawa, R. K. Chutani, C. Gorecki, R. Boudot, P. Dziuban, V. Giordano, S. Clatot, and L. Mauri, Sens. Actuators, A **167**, 594 (2011).
[16]W. Yang, D. B. Conkey, B. Wu, D. Yin, A. R. Hawkins, and H. Schmidt, Nature Photon. **1**, 331 (2007).
[17]L. Liew, S. Knappe, J. Moreland, H. Robinson, L. Hollberg, and J. Kitching, Appl. Phys. Lett. **84**, 2694 (2004).
[18]M. Arditi and T. R. Carver, Phys. Rev. **136**, A643 (1964).
[19]M. Auzinsh, D. Budker, and S. M. Rochester, *Optically Polarized Atoms* (Oxford University Press, New York, 2010).
[20]P. Böhi, M. F. Riedel, J. Hoffrogge, J. Reichel, T. W. Hänsch, and P. Treutlein, Nat. Phys. **5**, 592 (2009).
[21]T. Pfau, University of Stuttgart, private communication (2012).
[22]M. D. Rotondaro and G. P. Perram, J. Quant. Spectrosc. Radiat. Transf. **57**, 497 (1997).
[23]P. Siddons, C. Adams, C. Ge, and I. Hughes, J. Phys. B **41**, 155004 (2008).
[24]S. J. Seltzer and M. V. Romalis, J. Appl. Phys. **106**, 114905 (2009).